Effects of Flow History on Oil Entrapment in Porous Media: An Experimental Study

Homa Khosravian, Vahid Joekar-Niasar, and Nima Shokri
School of Chemical Engineering and Analytical Science, Faculty of Engineering and Physical Sciences, University of Manchester, Manchester, U.K.

DOI 10.1002/aic.14708
Published online December 21, 2014 in Wiley Online Library (wileyonlinelibrary.com)

The effect of flow history on fluid phase entrapment during immiscible two-phase flow in Hele-Shaw cells packed with spherical and crushed glass beads is investigated. The wetting fluid is injected into an initially oil saturated cell at a well-defined capillary number. It is observed that the size and shape of the trapped clusters strongly depend on the history of flooding such that less oil was trapped in the medium when the injecting capillary number gradually increased to the final maximum capillary number compared to the case when the injection was started and maintained constant at the maximum capillary number. In addition, a comprehensive series of experiments were conducted to delineate the effects of the capillary number on the phase entrapment. Contrary to previously published data, our experimental data reveal that the residual oil saturation depends on capillary number nonmonotonically. A physically based relationship to scale the capillary desaturation curve is proposed. © 2014 American Institute of Chemical Engineers *AIChE J*, 61: 1385–1390, 2015
Keywords: interfacial processes, multiphase flow, phase entrapment, capillary desaturation curve

Introduction

The classical approach to model two-phase flow in porous media involves mass and momentum balance equations based on Darcy's law for each phase and a relationship between pressures of the phases and saturation referred to as "capillary pressure curve."[1,2] The permeability for each phase is modeled through the relative permeability function. Both relative permeability and capillary pressure curves are a nonlinear hysteretic function of saturation.[2] In both of these constitutive functions, the residual phase saturations are important parameters obtained experimentally. During immiscible displacement of a receding fluid by an invading fluid in porous media disconnected fluid clusters trapped in the porous structure may be created due to the interplay among capillary, gravity and viscous forces. In practice, the contribution of the discontinuous phase can be economically very important, since during oil production, a part of it may be trapped in the reservoir, forming a discontinuous phase in the swept zone that may occupy 25% to 50% of the pore space after secondary oil production.[3]

Depending on flow regime controlled by the gravity, viscous and capillary force balance, different invasion patterns can be created leading to different residual saturations.[4–6] There are many models proposed for trapped phase saturation under different boundary conditions as discussed in Joekar-Niasar et al.[7] Tanino and Blunt[8] investigated the effect of wettability on the amount of trapped phase during imbibition under different wettability conditions. Recently, Krummel et al.[9] investigated the effect of pore-scale fluid dynamics on ganglia configuration. Their results illustrate that the amount of trapped oil in a porous medium depends on the competition between capillary and viscous forces within the media as expected. They showed how pore-scale fluid dynamics affect the trapped fluid configurations in multiphase flow through three-dimensional (3-D) porous media using confocal microscopy. Effects of several parameters such as viscosity ratio, particle sizes, wettability, and displacement rate on the phase entrapment were investigated in the past.[10–12] Reviewing the previous papers on this topic is beyond the scope of this work and the interested readers are referred to Sahimi[2] for a comprehensive list of literature on this topic.

Despite of the extensive research on describing the residual saturation under a given boundary condition, the effect of the flow history on the phase entrapment has been rarely investigated in the past which constitutes the key objectives of this article. Motivated by important applications of immiscible two-phase flow in porous media, the key objectives of this article are to delineate (a) the effects of the history of wetting fluid injection on the phase entrapment during imbibition in porous media and (b) the relation between capillary number (defined as the ratio of viscous to capillary forces) and residual saturation. We conducted a comprehensive series of imbibition experiments using Hele-Shaw cells packed with spherical and crushed glass beads saturated with two different types of oil which will be described in detail in following sections.

Experimental Considerations

All experiments were carried out in quasi-2-D horizontal transparent Hele-Shaw cells. Two cells were used in the experiments with the dimension of 0.1 m in length and 0.1 m in width and thicknesses of 0.003 and 0.004 m.

Correspondence concerning this article should be addressed to N. Shokri at nima.shokri@manchester.ac.uk.

Injection and production ports at opposite sides of the cells were drilled to control the inlet and outlet flux. Spherical and crushed glass beads with sizes ranging from 0.5 to 1.0 mm were used as model porous media. The following steps were taken to prepare and pack the Hele-Shaw cells: (a) glass beads were poured in a bottle filled with the nonwetting fluid (Soltrol 220 from ChemPoint or Perchloroethylene [PCE] from SigmaAldrich); (b) the glass cell was filled with oil through an open cross section at the upmost part of the cell while the outlet was closed; (c) glass beads were carefully removed from the bottle filled with oil and packed inside the cell gradually until the cell was fully packed with the beads; (d) finally, the upmost open section was covered and completely sealed by a customized Plexiglas block which had four ports serving as the inlet to the Hele-Shaw cell. The packed cell was then placed horizontally to run the experiment. The same procedure was repeated in all experiments.

Using a syringe pump (World Precision Instruments) the displacing fluid was injected into the cell through four inlets with interval distance of 0.02 m. In all experiments, the displacing wetting fluid was dyed water (with 0.05% Nirgosine). Two types of oils were used in our experiments as the nonwetting fluids which were Soltrol 220 with the dynamic viscosity and density of 3.98 mPa s[13] and 794.5 kg/m^3, respectively resulting in the oil to water viscosity ratio of about 4.5. The second oil was PCE with the dynamic viscosity and density of 0.89 mPa s and 1622 kg/m^3, respectively, resulting in the oil to water viscosity ratio of 1 at 25 °C. Dyed water was injected into the Hele-Shaw cell at different flow rates (0.1, 1, 3, 5, 10, 30, 45, 60, 90 mL/h). Outlet flow was collected in a beaker mounted on a digital balance to record the displaced mass. Two series of experiments were conducted in this study.

In the first series, imbibition experiments were conducted to evaluate the effects of the flooding history on the residual saturation. To do so, the initial injection rate in each experiment was set at a different value which was gradually increased to the final injection rate of 90 mL/h which was the same in all experiments. During each round of the experiment, injection of the displacing fluid was continued until steady state was reached, that is, no more change in the phase distributions was observed. At that point, the injection rate was increased and the flooding was sustained with a higher flow rate to reach to a new steady-state condition. This procedure was repeated until the maximum designed capillary number. The patterns and distribution of trapped oil phase was investigated using the recorded images as a function of the flooding history.

In the second series of the experiments, the relation between the capillary number and the oil residual saturation was investigated. The displacing fluid was injected into the Hele-Shaw cell saturated with oil at different flow rate and the final oil residual saturation was computed (using image analysis) as a function of the injecting capillary number.

Image requisition and analysis

A Genie TS camera (Stemmer Imaging) controlled automatically by a computer was mounted vertically on top of the sample to capture the dynamics of oil and water distributions during the imbibition experiments. A lightbox was placed underneath the sample to insure uniform and homogenous illumination. The output images were 8-bit grayscale images with 2560 × 2048 pixels resulting in the spatial resolution of 0.04 mm per pixel. To quantify the patterns and morphology of phase distributions during imbibition experiments, the gray-scale images were segmented into black and white images indicating the water and oil saturated regions, respectively. Customized codes in MATLAB were developed for image segmentation. The segmentation algorithm has been presented in other studies (see for example Norouzi Rad and Shokri[14] and Shokri and Sahimi[15]). We used the same algorithm with some minor modifications as follows: the regions saturated with water and oil were clearly represented by two main "peaks" in the gray value histogram of each image. The first and second peak corresponded to the region saturated with the dyed water and oil, respectively. A threshold was applied to classify gray values as water or oil-filled zones. To determine the threshold, the derivative of the histogram was calculated and the threshold value was attributed to the point at which the derivative changed from a negative value to a positive one (essentially indicating the point at which the derivative is close or equal to zero). Figure 1 illustrates three images before and after segmentation. The black and white images were used to quantify the dynamics of oil/water displacement together with the residual oil saturation under different boundary conditions.

Results and Discussion

It is worthy to mention that each experiment in which spherical glass beads were used to pack the Hele-Shaw cell was generally repeated 2–5 times to ensure the reproducibility of the results but the experiment with the crushed glass was performed only once due to the material limitation.

Effects of flow history on the residual saturation

In the first series of experiments, the injecting capillary number was varied from 1.5×10^{-5} to 2.8×10^{-4}. Figure 2 qualitatively shows the final residual oil distribution at any given capillary number. Each row in Figure 2 corresponds to a separate round of experiment. The first image in each row corresponds to the phase distribution at the steady-state condition when the injection rate is the lowest. The subsequent images in each row illustrate the steady-state phase distribution at higher injection rates with the capillary number indicated at top. Note that the injection rate in each vertical column in Figure 2 is the same. This confirms qualitatively that patterns and the amount of the trapped oil at any given capillary number strongly depends on the injection history. Using the segmented images, the effect of the injection history on the phase entrapment is quantified. The results are presented in Figure 3 illustrating that less oil is trapped in the medium when the injection starts with a lower rate and gradually increases to the ultimate high injection rate compared to the case when the injection starts and remains constant at the final high injection rate. Besides, Figure 3 reveals that the effect of flow history is more substantial at lower capillary numbers. In the other word, when the final capillary number Ca_f increases the effect of flow history on the amount of trapped oil decreases.

Relation between the capillary number and residual oil saturation

The images on the main diagonal of Figure 2 qualitatively indicate that the residual oil saturation is not monotonically decreasing as the capillary number increases. This result is

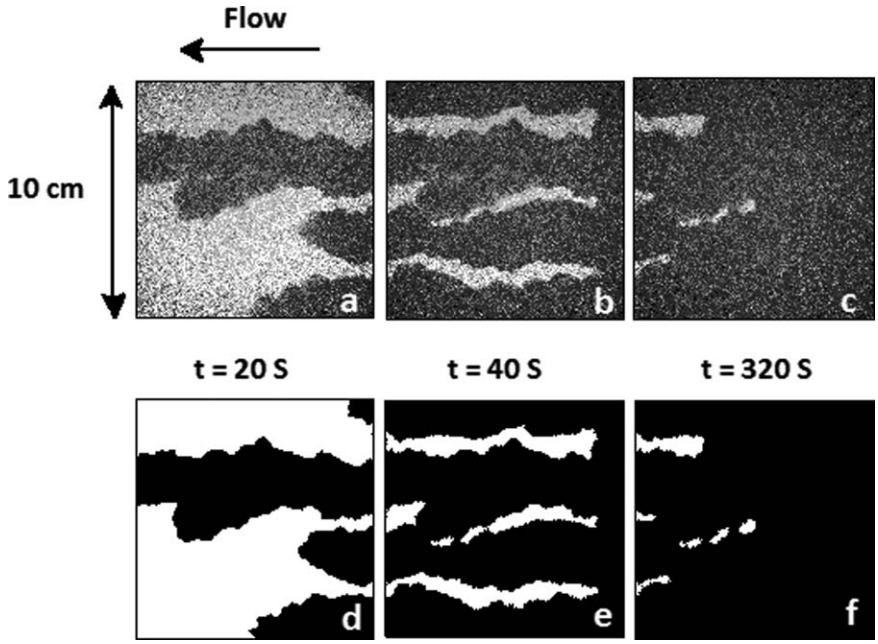

Figure 1. Three typical gray level images segmented into black and white images.

(a), (b), and (c) present the gray-scale image with the dark and light gray corresponding to dyed water and oil respectively. (d), (e), and (f) illustrate the segmented images with black and white indicating dyed water and oil, respectively. The injection was from right to left. The numbers indicate elapsed time from the onset of the experiment.

not trivial as previous studies reported a monotonic decrease of the residual saturation as capillary number increases.[2,16] For example, Dullien[16] showed the presence of a monotonic nonlinear relation between the capillary number and residual saturation that depended on the viscosity ratio.

To further investigate the observed nonmonotonic relation between the capillary number and residual oil saturation, we conducted the second series of experiments as mentioned before. To do so, a comprehensive series of imbibition experiments were conducted under different boundary conditions to obtain the capillary desaturation curve (CDC). The results are presented in Figure 4. This figure consists of four

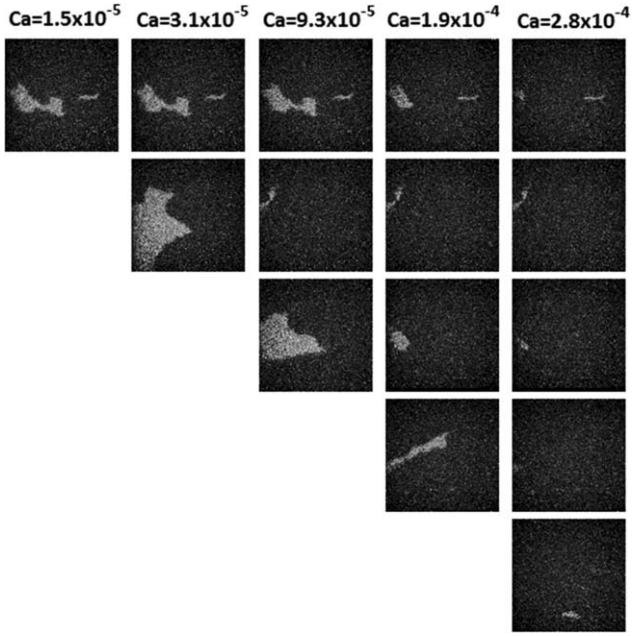

Figure 2. Images of the phase distributions at the steady-state condition (when no more change in phase distribution was observed).

The dark and light gray corresponds to the regions filled with water and oil, respectively. The first image in each row indicates the phase distribution at the steady-state condition when the injection rate is the lowest. The subsequent images in each row illustrate the steady-state phase distribution at higher injection rates with the corresponding capillary number values indicated at top. Results confirm the dependency of the phase distribution at any given capillary number on the initial injection rate and in general the history of flooding.

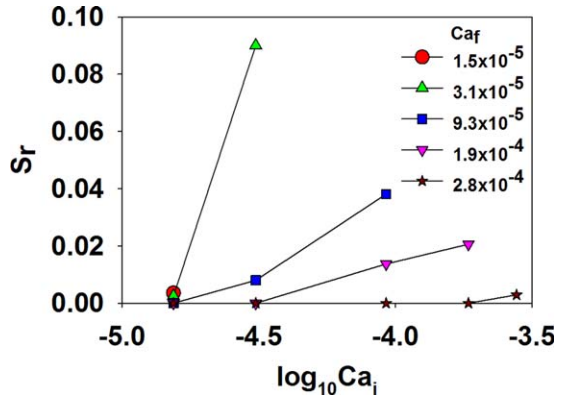

Figure 3. Effects of the history of flooding on oil entrapment.

The legend indicates the final capillary number Ca_f and Ca_i corresponds to the initial capillary number used to inject water into the medium at the onset of the experiment. Each point indicates a separate experiment started with the corresponding Ca_i and terminated when the injection rate reached to the final capillary number presented in the legend. S_r corresponds to the residual oil saturation at the steady-state condition when the capillary number was equal to Ca_f. In all experiments, the oil was Soltrol 220 (with the viscosity ratio of 4.5) and spherical glass beads were used to pack the Hele-Shaw cell. [Color figure can be viewed in the online issue, which is available at wileyonlinelibrary.com.]

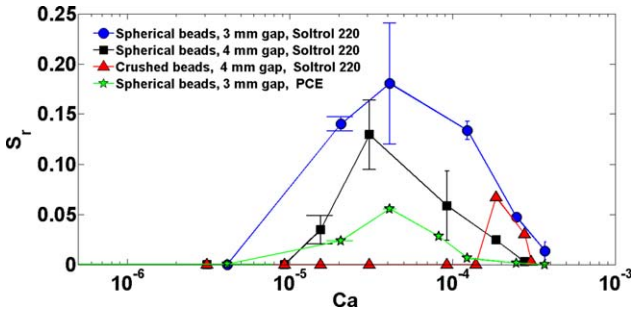

Figure 4. Variation of the residual oil saturation S_r through spherical and crushed glass beads as a function of the capillary number.

Two flow cells were used in the experiments with the thickness of 3 and 4 mm. Also, two types of oils were used in the experiments with the viscosity ratios (defined as the ratio of the viscosity of oil to water) of 4.5 and 1 in the case of Soltrol 220 and PCE, respectively. The errorbars indicate the standard deviation of the measured data. [Color figure can be viewed in the online issue, which is available at wileyonlinelibrary.com.]

sets of data namely: water displacing Soltrol 220 through the cell with the thickness of 3 and 4 mm packed with spherical glass bead (with particle sizes ranging between 0.5 and 1.0 mm); water displacing Soltrol 220 through the cell with the thickness of 4 mm packed with crushed beads; and finally, water displacing PCE through the cell with the gap thickness of 3 mm packed with spherical glass beads (with particle sizes ranging between 0.5 and 1.0 mm). Our results confirm a nonmonotonic relation between the residual saturation and capillary number of the displacing fluid under all aforementioned conditions.

Figure 4 indicates that at low capillary numbers, the residual saturation may increase as the capillary number increases up to a certain threshold (which was observed under different boundary conditions). Such behavior has been rarely reported in literature. We attribute the observed pattern to the local geometry of the packed beads used in our experiments. Although in our experiments, the porous medium was randomly packed in the cell, it remained relatively homogenous due to the narrow particle size ranges. At low capillary numbers, the capillary forces control the invasion. However, due to homogenous pore-size distribution and the quasi 2-D medium, the water may imbibe homogeneously with a stable front which will reduce trapping significantly. With increase of flow rate under unfavorable viscosity ratio, viscous forces will induce flow through more permeable zone that would lead to trapped phase behind the invasion front. At higher capillary numbers ($Ca > 5 \times 10^{-5}$), the amount of trapped phase decreases with increase of capillary number due to the mobilization of the trapped oil. This part of results has been already observed by several authors.[2,17–19]

In addition, Figure 4 shows less oil entrapment as viscosity ratio decreases (i.e. less entrapment when oil is less viscous). This conclusion is in line with the results of previous studies. For example, Vizika et al.[17] investigated the effect of viscosity ratio on the residual saturation during imbibition at low capillary numbers and showed that even for very small capillary numbers residual saturation significantly decreases when viscosity ratio decreases. Dias and Payatakes[18] also reported decrease of residual saturation as viscosity ratio decreases and capillary number increases.

The curves shown in Figure 4 pose the possibility of presenting all data in a single curve if the parameters are defined properly. All the experimental data in Figure 4 show no trapped phase under the two extreme ends of capillary numbers. Therefore, the general form should be proposed such that it guarantees zero trapped saturation under very small and very high capillary numbers. Based on these observations, we propose the following equation relating the saturation to the capillary number expressed as

$$S = S_{\max}\exp\left[-a(\mathrm{Ca}-\mathrm{Ca}_{\mathrm{cr}})^2/\mathrm{Ca}\right] \tag{1}$$

where $S_{\max}$ denotes the maximum trapped phase saturation, $\mathrm{Ca}_{\mathrm{cr}}$ denotes the critical capillary number where the maximum trapped phase saturation is obtained, Ca is the capillary number and "a" is a fitting parameter. This relation has been fit to the experimental data to obtain the values of $S_{\max}$, $\mathrm{Ca}_{\mathrm{cr}}$ and "a." The obtained parameters are listed in Table 1.

The capillary number measured in the laboratory is based on the macroscopic definition of capillary number. However, few studies[20–23] showed the importance of the pore-scale topology of trapped phase on its mobility. It has been shown that mobilization of a trapped phase occurs at the critical capillary number equal to 1 if defined based on microscale properties. Based on the microscale definition of capillary number, Eq. 1 can be rearranged as

$$\frac{S}{S_{\max}} = \exp\left[-\frac{a(\mathrm{Ca}_{\mathrm{micro}}-1)^2}{\mathrm{Ca}_{\mathrm{micro}}}\right] \tag{2}$$

where $\mathrm{Ca}_{\mathrm{micro}} = \mathrm{Ca}/\mathrm{Ca}_{\mathrm{cr}}$. Using Eq. 2, our experimental results have been scaled as shown in Figure 5 presenting the change of $S/S_{\max}$ vs. $\mathrm{Ca}/\mathrm{Ca}_{\mathrm{cr}}$ under different conditions. Interestingly, all data obtained in our experiments could be presented by almost a single curve described by Eq. 2.

Breakthrough time as influenced by the capillary number

Breakthrough times of the dyed water t_b defined as the first time that dyed water reached the outlet of the cell at different capillary numbers are shown in Figure 6. Our results confirm the presence of a scaling relation between the capillary number and the breakthrough time expressed as $t_b\ \mathrm{Ca}^{\alpha}$ with α indicating the scaling exponent. Interestingly, the measured data under different boundary conditions (different oils, types of grains, and the thickness of the Hele-Shaw cells) all are scaled with the capillary number using a single relation with the exponent of -0.95. Tallakstad et al.[24] and Zhu and Papadopoulos[25] observed power law relations

Table 1. The Parameters Computed by Fitting of Eq. 1 on the Experimental Data Measured in Each Round of the Experiment

Boundary Conditions	a	$\mathrm{Ca}_{\mathrm{cr}}$	$S_{\max}$
Spherical beads, 3-mm gap, Soltrol 220	1.46×10^4	5.59×10^{-5}	0.28
Spherical beads, 4-mm gap, Soltrol 220	4.69×10^4	4.65×10^{-5}	0.11
Crushed beads, 4-mm gap, Soltrol 220	2.03×10^4	4.65×10^{-5}	0.21
Spherical beads, 4-mm gap, PCE	3.72×10^4	4.25×10^{-5}	0.05

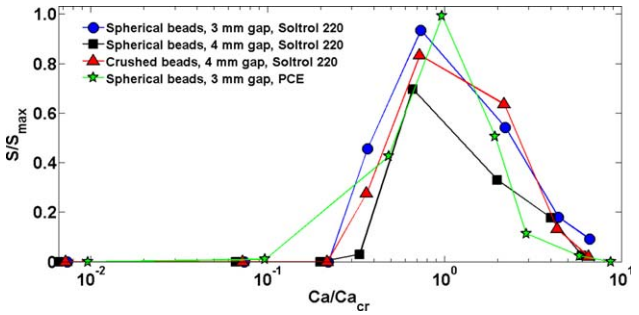

Figure 5. Physically based scaling of capillary desaturation curve.

The legend indicates the same as in Figure 4. [Color figure can be viewed in the online issue, which is available at wileyonlinelibrary.com.]

between the breakthrough time and capillary numbers too with −0.89 and −1.54 as exponents of the power law respectively. Zhu and Papadopoulos[25] discussed that the difference in the reported exponents is due to the difference in experimental conditions as they conducted drainage experiments on a freshly packed microchannels while Tallakstad et al.[24] performed experiments on a quasi-2-D Hele Shaw cell with coinjection of wetting and nonwetting fluid into a sample which was initially saturated with wetting fluid. The exponent obtained in our experiments differs from the previously reported values. Although in this work the Hele-Shaw cell was randomly packed with the glass beads, it may behave as a homogenous medium due to the relatively narrow range of particle sizes. The small deviation of the scaling exponent from 1 confirms that the porous medium used in this work is a relatively homogenous medium and has properties very close to a simple cylindrical tube with no porous medium in which the capillary resistance is negligible.

Summary and Conclusions

A comprehensive series of imbibition experiments were performed to study the history of flooding and its role in oil displacement during imbibition in a quasi-2-D porous medium and also to delineate the relation between the capillary number and oil entrapment. The porous medium was prepared by randomly packing a Hele-Shaw cell with 0.5–1 mm spherical and crushed glass beads. Soltrol 220 and PCE were used as the high and low viscous nonwetting fluid. In all experiments, dyed water was the invading wetting fluid. The results show that the size and pattern of the trapped oil during oil recovery strongly depend on the history of flooding. Our results show that less oil is trapped in the medium if the injection starts from a low capillary number that gradually increases to the high and ultimate injection capillary number. It was also shown that the history dependency of the residual oil saturation decreases as the capillary number increases. Moreover, at low capillary numbers ($Ca < 10^{-5}$) very efficient oil recovery was observed which was due to the relatively homogeneous porous medium used in this work. Besides, a nonmonotonic relation between the injection capillary number and the residual saturation was observed under different boundary conditions. We have proposed an equation which was used to describe different CDCs. Using the proposed equation, all experimental data measured in our study under different boundary conditions could be presented on a single curve. Additionally, the relation between capillary numbers and breakthrough times observed in all experiments could be described by a single power law with an exponent of −0.95. This is likely due to the relatively homogenous porous media used in our experiments leading to the behavior close to what is expected from a cylindrical tube with no porous medium.

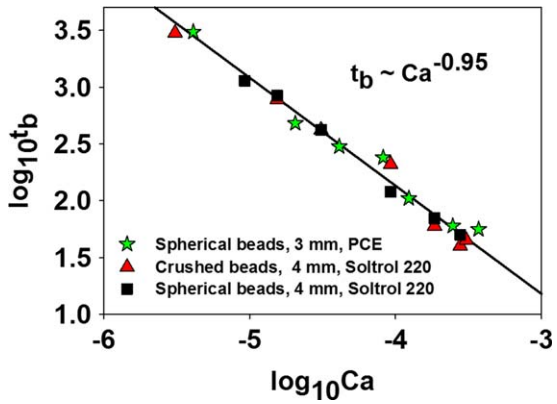

Figure 6. Breakthrough times t_b as a function of the capillary number.

In all cases, t_b is scaled with the capillary number using a single power law with the exponent of −0.95. [Color figure can be viewed in the online issue, which is available at wileyonlinelibrary.com.]

Acknowledgment

Acknowledgment is made to the donors of the American Chemical Society Petroleum Research Fund (ACS-PRF) for support of this research (PRF 52054-DNI6).

Literature Cited

1. Joekar-Niasar V, Hassanizadeh SM, Dahle HK. Non-equilibrium effects in capillarity and interfacial area in two-phase flow: dynamic pore-network modeling. *J Fluid Mech*. 2010;655:38–71.
2. Sahimi M. *Flow and Transport in Porous Media and Fractured Rock: From Classical Methods to Modern Approaches*, *2nd ed*. Weinheim: Wiley-VCH Publishers, 2011.
3. Payatakes AC. Dynamics of oil ganglia during immiscible displacement in water-wet porous media. *Ann Rev Fluid Mech*. 1982;14:365–393.
4. Wilkinson D. Percolation model of immiscible displacement in the presence of buoyancy forces. *Phys Rev A*. 1984;30(1):520.
5. Lenormand R, Zarcone C. Invasion percolation in an etched network: Measurement of a fractal dimension. *Phys Rev Lett*. 1985;54(20):2226.
6. Oxaal U, Murat M, Boger F, Aharony A, Feder J, Jøssang T. Viscous fingering on percolation clusters. *Nature*. 1987;329(3):32–37.
7. Joekar-Niasar V, Doster F, Armstrong RT, Wildenschild D, Celia MA. Trapping and hysteresis in two-phase flow in porous media: a pore-network study. *Water Resour Res*. 2013;49:4244–4256.
8. Tanino Y, Blunt MJ. Laboratory investigation of capillary trapping under mixed-wet conditions. *Water Resour Res*. 2013;49:4311–4319.
9. Krummel AT, Datta SS, Münster S, Weitz DA. Visualizing multiphase flow and trapped fluid configurations in a model three-dimensional porous medium. *AIChE J*. 2013;59(3):1022–1029.
10. Abrams A. Influence of fluid viscosity, interfacial tension, and flow velocity on residual oil saturation left by waterflood. *Soc Pet Eng J*. 1975;15:437–447.
11. Sahimi M. Flow phenomena in rocks: from continuum models tofractals, percolation, cellular automata, and simulated annealing. *Rev Mod Phys*. 1993;65(4):1393–1534.
12. Yiotis AG, Talon L, Salin D. Blob population dynamics during immiscible two-phase flows in reconstructed porous media. *Phys Rev E*. 2013;87:033001.

13. Zhou X, Morrow NR, Ma S. Interrelationship of wettability, initial water saturation, aging time, and oil recovery by spontaneous imbibition and waterflooding. *Soc Pet Eng J*. 2000;5(2): 199–207.
14. Norouzi Rad M, Shokri N. Nonlinear effects of salt concentrations on evaporation from porous media. *Geophys Res Lett*. 2012;39: L04403.
15. Shokri N, Or D. Drying patterns of porous media containing wettability contrasts. *J Colloid Interface Sci*. 2013;391:135–141.
16. Dullien FAL. *Porous Media Fluid Transport and Pore Structure, 2nd ed*. San Diego: Academic, 1992.
17. Vizika O, Avraam DG, Payatakes AC. On the role of viscosity ratio during low- capillary-number forced imbibition in porous media. *J Colloid Interface Sci*. 1994;165:386–401.
18. Dias MM, Payatakes AC. Network models for two-phase flow in porous media part 1. Immiscible microdisplacement of non-wetting fluids. *J Fluid Mech*. 1986;164:305–336.
19. Dias MM, Payatakes AC. Network models for two-phase flow in porous media part 2. Motion of oil ganglia. *J Fluid Mech*. 1986;164: 337–358.
20. Hilfer R, Øren PE. Dimensional analysis of pore scale and field scale immiscible displacement. *Transp Porous Media*. 1996;22: 53–72.
21. Joekar-Niasar V, Hassanizadeh SM. Uniqueness of specific interfacial area–capillary pressure–saturation relationship under non-equilibrium conditions in two-phase porous media flow. *Transp Porous Media*. 2012;94:465–486.
22. Armstrong RT, Georgiadis A, Ott H, Klemin D, Berg S. Critical capillary number: desaturation studied with fast X-ray computed microtomography. *Geophys Res Lett*. 2014;41:55–60.
23. Melrose JC, Brandner CF. Role of capillary forces in determining microscopic displacement efficiency for oil recovery by waterflooding. *J Can Pet Technol*. 1974;13(4):54–62.
24. Tallakstad KT, Løvoll G, Knudsen HA, Ramstad T, Flekkøy EG, Måløy KJ. Steady-state, simultaneous two-phase flow in porous media: an experimental study. *Phys Rev E*. 2009;80:036308.
25. Zhu P, Papadopoulos KD. Visualization and quantification of two-phase flow in transparent miniature packed beds. *Phys Rev E*. 2012; 86:046313.

Manuscript received Aug. 30, 2014, and revision received Nov. 13, 2014.